



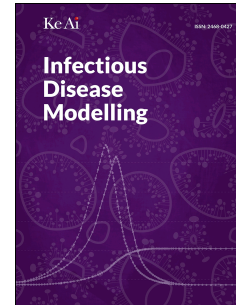
Since January 2020 Elsevier has created a COVID-19 resource centre with free information in English and Mandarin on the novel coronavirus COVID-19. The COVID-19 resource centre is hosted on Elsevier Connect, the company's public news and information website.

Elsevier hereby grants permission to make all its COVID-19-related research that is available on the COVID-19 resource centre - including this research content - immediately available in PubMed Central and other publicly funded repositories, such as the WHO COVID database with rights for unrestricted research re-use and analyses in any form or by any means with acknowledgement of the original source. These permissions are granted for free by Elsevier for as long as the COVID-19 resource centre remains active.

Journal Pre-proof

Modeling the impact of surveillance activities combined with physical distancing interventions on COVID-19 epidemics at a local level

Guan-Jhou Chen, John R.B. Palmer, Frederic Bartumeus, Ana Alba Casals



PII: S2468-0427(22)00084-7

DOI: <https://doi.org/10.1016/j.idm.2022.11.001>

Reference: IDM 333

To appear in: *Infectious Disease Modelling*

Received Date: 28 July 2022

Revised Date: 26 October 2022

Accepted Date: 3 November 2022

Please cite this article as: Chen G.-J., Palmer J.R.B., Bartumeus F. & Casals A.A., Modeling the impact of surveillance activities combined with physical distancing interventions on COVID-19 epidemics at a local level, *Infectious Disease Modelling* (2022), doi: <https://doi.org/10.1016/j.idm.2022.11.001>.

This is a PDF file of an article that has undergone enhancements after acceptance, such as the addition of a cover page and metadata, and formatting for readability, but it is not yet the definitive version of record. This version will undergo additional copyediting, typesetting and review before it is published in its final form, but we are providing this version to give early visibility of the article. Please note that, during the production process, errors may be discovered which could affect the content, and all legal disclaimers that apply to the journal pertain.

© 2022 The Authors. Publishing services by Elsevier B.V. on behalf of KeAi Communications Co. Ltd.

1 **Modeling the impact of surveillance activities combined with**
2 **physical distancing interventions on COVID-19 epidemics at a**
3 **local level**

4 Guan-Jhou Chen^{a,b}, John R.B. Palmer^c, Frederic Bartumeus^{d,e,f}, Ana Alba Casals^g,

5

6 ^aCollege of Medicine, National Taiwan University, Taipei, Taiwan

7 ^bMin-Sheng General Hospital, Taoyuan, Taiwan

8 ^cDepartment of Political and Social Sciences, Universitat Pompeu Fabra, Barcelona, Spain

9 ^dCentre d'Estudis Avançats de Blanes (CEAB-CSIC), Blanes 17300, Spain

10 ^eCentre de Recerca Ecològica i Aplicacions Forestals (CREAF), Cerdanyola del Vallès 08193,
11 Spain

12 ^fInstitució Catalana de Recerca i Estudis Avançats (ICREA), Barcelona 08010, Spain

13 ^gCentre de Recerca en Sanitat Animal (CRESA), Institut de Recerca i Tecnologia
14 Agroalimentàries, Spain

15

16

17 **Word count**

18 Abstract: 250

19 Text: 4273

20

21 ***Corresponding author:** Ana Alba Casals, PhD

22 Centre de Recerca en Sanitat Animal (CRESA), Institut de Recerca i Tecnologia

23 Agroalimentàries, Spain

24 E-mail: casalsalbaanna@gmail.com

25 TEL: +34-972-701-181

Journal Pre-proof

1 **Abstract**

2 Physical distancing and contact tracing are two key components in controlling
3 the COVID-19 epidemics. Understanding their interaction at local level is
4 important for policymakers. We propose a flexible modeling framework to assess
5 the effect of combining contact tracing with different physical distancing
6 strategies. Using scenario tree analyses, we compute the probability of COVID-19
7 detection using passive surveillance, with and without contact tracing, in
8 metropolitan Barcelona. The estimates of detection probability and the frequency
9 of daily social contacts are fitted into an age-structured susceptible-exposed-
10 infectious-recovered compartmental model to simulate the epidemics considering
11 different physical distancing scenarios over a period of 26 weeks. With the original
12 Wuhan strain, the probability of detecting an infected individual without
13 implementing physical distancing would have been 0.465, 0.515, 0.617, and 0.665
14 in designated age groups (0-14, 15-49, 50-64, and >65), respectively. As the
15 physical distancing measures were reinforced and the disease circulation
16 decreased, the interaction between the two interventions resulted in a reduction
17 of the detection probabilities; however, despite this reduction, active contact
18 tracing and isolation remained an effective supplement to physical distancing. If
19 we relied solely on passive surveillance for diagnosing COVID-19, the model

20 required a minimal 50% (95% credible interval, 39-69%) reduction of daily social
21 contacts to keep the infected population under 5%, as compared to the 36% (95%
22 credible interval, 22-56%) reduction with contact tracing systems. The simulation
23 with the B.1.1.7 and B.1.167.2 strains shows similar results. Our simulations showed
24 that a functioning contact tracing program would reduce the need for physical
25 distancing and mitigate the COVID-19 epidemics.

26

27 **Keywords:** SARS-CoV-2, physical distancing, social mixing pattern, contact tracing,
28 scenario tree analysis.

29

30 **1. Introduction**

31 In 2019, human cases of coronavirus disease 2019 (COVID-19) caused by
32 severe acute respiratory syndrome coronavirus 2 (SARS-CoV-2) were first reported
33 in Wuhan, China (Guan et al., 2020; Zhu et al., 2020). SARS-CoV-2 can result in
34 pneumonia and respiratory distress, among other severe clinical signs, especially
35 in elderly patients and those with comorbidities (Guan et al., 2020; Redondo-Bravo
36 et al., 2020; Thakur et al., 2021; Wang et al., 2020; Yang et al., 2020). Following its
37 emergence in China, the virus rapidly spread across all continents, resulting in a
38 pandemic unprecedented in recent history. The rapid surge of COVID-19 cases
39 overwhelmed healthcare systems in many countries and resulted in high excess
40 mortality (Thakur et al., 2021). As the pandemic unfolded, various strategies were
41 proposed and implemented by different authorities to mitigate its impact, first
42 prior to and then later in combination with vaccination campaigns (Anderson,
43 Heesterbeek, Klinkenberg, & Hollingsworth, 2020).

44 Among these strategies, one of the mainstays has been physical distancing
45 (often known as social distancing), which aims to encourage a minimum physical
46 distance and reduce the frequency of contacts between people (Chu et al., 2020).
47 In order to reduce the frequency of contacts, many authorities have introduced
48 restrictions on social activities, such as suspending public gatherings, closing

49 schools, teleworking, limiting long-distance movements, and so on. Social mixing
50 studies conducted before and after the spread of COVID-19 have demonstrated
51 how the frequency of daily social contacts was reduced by these measures. In
52 Spain, web-based survey research reveals a lower number of daily social contacts
53 when physical distancing measures were imposed during the pandemic compared
54 to pre-COVID estimates of contacts in southern Europe (Mossong et al., 2008;
55 Palmer, Ottow, & Bartumeus, 2021). In the CONNECT study from Québec, Canada,
56 the daily social contacts were reduced by around 50% due to various
57 governmental restrictions when compared to pre-COVID era (Brisson et al., 2021).

58 Apart from physical distancing, prompt diagnosis and isolation of infectious
59 individuals have also been deemed critical for the control of different infectious
60 diseases, including COVID-19 (Girum, Lentiro, Geremew, Migora, & Shewamare,
61 2020; Saurabh & Prateek, 2017). Therefore, in addition to passive surveillance, in
62 which diagnostic tests are performed based on clinical suspicion of COVID-19
63 cases, countries have taken various active approaches to detecting cases. One of
64 the most common approaches is the combination of a disease notification system
65 and contact tracing. After positive cases are reported to public health authorities,
66 depending on the severity of infection and the availability of resources, these
67 cases are isolated in different settings (intensive care units [ICU], hospital wards,

68 quarantine facilities, home isolation, etc.) and authorities track and quarantine
69 their contacts to prevent further transmission (Girum et al., 2020; Kucharski et al.,
70 2020). A well-established notification and contact tracing system can mitigate the
71 transmissibility of infectious diseases. First, reported infectious cases can be
72 isolated to prevent further transmission. Depending on the timeliness of contact
73 tracing, secondary cases can be tracked and quarantined before becoming
74 infectious, avoiding onward transmission to others. Compliance with isolation and
75 quarantine measures directly impacts how the notification and contact tracing
76 system contributes to the mitigation of epidemics. Furthermore, contact tracing
77 should increase the probability of positive cases being diagnosed in the healthcare
78 system since people might be tracked and tested even if they are asymptomatic.

79 Many researchers have studied and modelled the impact of either contact
80 tracing systems or physical distancing measures on the dynamics of COVID-19
81 epidemics. However, the influence of the interplay between these two major
82 interventions at a local level is less described in the literature. For example,
83 limiting public gatherings or closing schools may alter the age distribution of an
84 individual's daily social contacts. Since the symptoms and severity of COVID-19 are
85 greatly influenced by the age of the infected, it is reasonable to assume that the
86 efficacy of contact tracing might change alongside different physical distancing

87 measures. Furthermore, if the average number of secondary cases is reduced due
88 to physical distancing measures, the chances of tracing back to the primary cases
89 might also be affected.

90 In this study, we develop a flexible modeling framework to estimate the
91 effectiveness of a contact tracing system and to represent the interplay between
92 physical distancing and contact tracing measures on COVID-19 dynamics at a local
93 level. To illustrate its applicability, we simulate the epidemic dynamics for different
94 COVID variants on the resident population of the metropolitan area of Barcelona
95 (Spain), considering the implementation of a contact tracing system and testing
96 the influence of various levels of physical distancing.

97

98 **2. Materials and methods**

99 We developed a modeling framework that combined scenario tree (ST)
100 analyses (Food and Agriculture Organization, 2014), which assessed the sensitivity
101 of surveillance actions, with an age-structured susceptible-exposed-infectious-
102 recovered (SEIR) compartmental model to simulate the dynamics of COVID-19
103 epidemics at the local level, accounting for mitigation measures such as physical
104 distancing.

105 The ST analysis is frequently employed to demonstrate freedom of disease in
106 animal disease surveillance (Food and Agriculture Organization, 2014). In this
107 work, ST analysis was used to evaluate the probability of detecting an infected
108 person according to his or her age using various potentially overlapping
109 surveillance system components such as passive surveillance and contact tracing.
110 The estimates of the ST analysis combined with other data, including the
111 demographics of the population (age structure, comorbidities), social contact
112 patterns, and natural history of disease, were used as inputs to fit a SEIR model.
113 This SEIR model simulates the epidemic dynamics for the residents of the
114 Barcelona metropolitan area over a period of 26 weeks, comparing three COVID
115 variants with different surveillance strategies and physical distancing interventions.
116 The conceptual and modelling framework are depicted in Figure 1.

117

118 **2.1. Estimating the detection probability of cases of COVID-19**

119 We used ST analysis to estimate the probability of detecting COVID-19 cases
120 according to the age category i combining surveillance components ($p.detect_i$).

121 Four age strata were designated: (0 to 14 years of age, 15 to 49, 50 to 64, and
122 above 65). In our study, the $p.detect_i$ comprised two components: passive
123 surveillance and contact tracing (either physical or digital). Other components of
124 surveillance, such as population-wide sampling or voluntary screening, were not
125 considered.

126 In passive surveillance, the detection probability depends on the probability
127 of presenting clinical symptoms, seeking healthcare, being tested during
128 consultation, and the sensitivity of diagnostic tests (Figure 2). The detection
129 probability by passive surveillance in each age stratum ($p.detect.pass_i$) equals the
130 product of the probabilities in each step.

131 In terms of contact tracing, we started by estimating the probability of a
132 COVID-19 case being 'traceable' by the contact tracing system ($p.traceable_i$) and
133 then we accounted for potential losses during the process of contact tracing, such
134 as incompliance, false negativity, etc. (Figure 3). The parameters used in the ST
135 analysis are listed in Table 1, and more details of the calculation are described in

136 Supplement 1.

137 Theoretically, contact tracing can be forward, in which secondary cases are
138 traced due to their contact with a primary case, or backward, when the primary
139 case is traced back after the diagnosis of secondary cases. Since the differentiation
140 might be challenging in reality, in our calculation, forward and backward tracing
141 were considered altogether. Furthermore, the means of contact tracing, either
142 traditionally or digitally, were not differentiated in the model. According to the
143 Spanish guidelines, exposed contacts would be notified by the public health
144 service once the primary case was diagnosed and they would be requested to be
145 quarantined at home for 10 days (Ministerio de Sanidad España, 2020).
146 Furthermore, a diagnostic test would be performed during the 10-day quarantine
147 period. In Spain, nucleic acid tests were required to confirm that an exposed
148 contact was not infected with SARS-CoV-2. Contacts who tested negative and
149 remained asymptomatic would be requested to finish the 10-day quarantine, while
150 those who developed clinical symptoms would be further managed and re-tested
151 as suspected cases (Ministerio de Sanidad España, 2020).

152 In the ST analysis, we inferred the age distribution of infected contacts to the
153 primary case by estimating the daily social contacts from each age stratum. We
154 used the projected contact matrix generated from the population-based contact

155 diaries of the POLYMOD study (Mossong et al., 2008; Prem, Cook, & Jit, 2017)
156 because there were no social mixing studies focusing on Barcelona or Spanish
157 residents prior to the COVID pandemic. This matrix was then weighted according
158 to the population age structure of the metropolitan area of Barcelona to generate
159 the baseline contact matrix (Table 2).

160

161 **2.2. Parameterizing the Effectiveness of Isolation**

162 Other considerations had to be taken into account while estimating the
163 effectiveness of isolation. First, the daily detection rate (γ_d) and the time to
164 detection ($1/\gamma_d$), which describe the transition of the status of individuals from the
165 'Infectious' compartment to the 'Isolated' compartment (see Figure S1). We
166 calculated the transition rate by using the probability-rate equation describing the
167 change between two states (Gidwani & Russell, 2020). The equation assumed that
168 the transition rate between the two states (in our case, from 'Infectious' to
169 'Isolated') was constant throughout the period of infectiousness. Once an
170 individual was moved into the 'Isolated' compartments, we assumed that this
171 individual remained isolated for the rest of the infectious period and the frequency
172 of daily social contacts was reduced by 50%.

173 As aforementioned, individuals might also be quarantined as infected

174 contacts since the beginning of their infection. The probability of exposed
175 contacts being identified and quarantined before becoming infectious (δ_e) could
176 be estimated based on the daily detection rate (γ_d) and the duration of the
177 'exposed' period ($1/\varepsilon$). The calculation of the values for these variables related to
178 the isolation procedure is listed in Table 1.

179

180 **2.3. Simulating the COVID-19 dynamics using a SEIR compartmental model**

181 The dynamics of COVID-19 epidemics was simulated by a stochastic SEIR
182 compartmental model adapted to the same four-age strata. The model was
183 created based on the structure proposed by Tuite et al. (Figure S1) and tailored to
184 the demographics, social interactions, and epidemiological data of the Barcelona
185 metropolitan area (Tuite, Fisman, & Greer, 2020). The demographics, the social
186 contact matrix and the epidemiological inputs used to fit the model are shown in
187 Table 2, Table S1 and S2. We also took into account the proportion of comorbid
188 conditions related to severe COVID-19 diseases such as cardiovascular diseases,
189 cerebrovascular diseases, obesity, diabetes mellitus, pulmonary diseases, and any
190 active cancers, based on data obtained from the Sistema d'Informació dels Serveis
191 d'Atenció Primària (SISAP), Institut Català de la Salut (ICS), Generalitat de
192 Catalunya (Table S2). To account for the uncertainty in real life, we included a

193 stochastic variable through a simulated realization of the Wiener process during
194 the calculation of the force of infection in the SEIR model (Szabados, 2010).

195 We hypothesized that all severe cases of COVID-19 would be diagnosed and
196 hospitalized, whereas the probability of detecting mild cases would depend on the
197 probability of detection ($p. detect_i$). Hospitalized severe patients were assumed to
198 have no contact with the community and the probability of transmission within
199 healthcare institutions was not included. Mild cases would be isolated after their
200 diagnosis. In the scenario of contact tracing, a proportion (calculated according to
201 the detection probability) of exposed contacts were regarded as isolated from the
202 start of their infection. The transmission related to isolated cases or contacts was
203 reduced due to the reduction of social contacts.

204 The model was run for 26 weeks (182 days), and we assumed that re-infection
205 during this period was not possible after the recovery of COVID-19. The model
206 described the general population in metropolitan Barcelona and the residents of
207 long-term care facilities were not considered. To estimate the maximum possible
208 requirements of ICU beds, we hypothesized that all critically ill patients would be
209 admitted to the ICU before death.

210

211 **2.4. Scenarios simulated and outputs of the model**

212 Firstly, we assessed how $p.detect_i$ would change with the strengthening of
213 physical distancing measures by reducing their daily social contacts from 100% of
214 baseline to 20%. Then, we simulated how overall attack rates, hospitalizations, ICU
215 admissions, and mortalities would change with the same strengthening of physical
216 distancing measures. Furthermore, to demonstrate the effectiveness of contact
217 tracing, we compared the required level of social contacts reduction to keep the
218 overall attack rates under designated thresholds of 5% and 2% within the model
219 period (26 weeks), which corresponded to the World Health Organization
220 epidemiological indicators of COVID-19 community transmission (WHO, 2021).

221 To represent the epidemic dynamics of the original Wuhan SARS-CoV-2
222 strain, the B.1.1.7 variant of concern (VOC), and the B.1.167.2 VOC, three different
223 basic reproduction numbers (R_0) were used in the simulation (Table S2).

224 The ST analyses and compartmental model were constructed using the R
225 language programming (version 3.6.3) and *RStudio* software, version 1.2.5001. The
226 calculation of the differential equations in the model was done by using the
227 *deSolve* package (Soetaert, Petzoldt, & Setzer, 2010). Overall attack rates, numbers
228 of hospitalizations, ICU admissions, and mortalities were projected in each age
229 stratum. For each simulated scenario, we repeated 200 iterations. The model
230 outputs were presented as the median values and credible intervals of the 200

231 iterations. We used 95% credible intervals to refer to the range of outcomes from
232 the 2.5th to 97.5th of percentiles. All the data used in our study was publicly
233 available data or anonymized aggregated data, and ethical review was not
234 required.
235

Journal Pre-proof

236 3. Results

237 3.1. Estimated Probability of Detection in Different Scenarios

238 With the scenario tree depicting passive surveillance (Figure 2) and related
239 variables (Table 1), using passive surveillance, we estimated that the probabilities
240 of detection per age class i ($p.detect.pass_i$) were 0.080 [0 – 14 years], 0.160 [15 –
241 49 years], 0.266 [50 – 64 years], and 0.365 [above 65 years]. Since the calculation
242 of passive surveillance depended on the clinical presentation of different age
243 strata, it would not change with the physical distancing measures or R_0 . When
244 combined with contact tracing, the overall probability of detection ($p.detect_i$)
245 would vary slightly according to the R_0 used in the calculation. With the R_0
246 representing the original Wuhan SARS-CoV-2 strain ($R_0 = 2.6$), the estimated
247 baseline $p.detect_i$ (without physical distancing) were 0.465, 0.515, 0.617, and
248 0.665 in the four age strata, respectively. With the B.1.1.7 VOC ($R_0 = 3.4$), the
249 estimated $p.detect_i$ were 0.493, 0.537, 0.637, and 0.680. Finally, with the B.1.167.2
250 VOC ($R_0 = 5.1$), the estimated $p.detect_i$ would further increase slightly to 0.510,
251 0.551, 0.649, and 0.689, respectively.

252 To represent the strengthening of physical distancing, the daily social contacts
253 were reduced gradually from allowing 100% of the baseline (indicating no physical
254 distancing measures in place) to only 20% (indicating an extreme level of physical

255 distancing). With this strengthening of physical distancing, the estimated
256 $p.detect_i$ also decreased gradually in the four age strata (Figure 4). For the
257 original Wuhan strain, the $p.detect_i$ with only 20% of baseline daily social
258 contacts allowed were 0.150, 0.225, 0.318 and 0.407; respectively. In our scenario
259 tree model, the decrease of $p.detect_i$ was non-linear and was less significant
260 when the R_0 was high.

261

262 **3.2. How Contact Tracing Impacts the Overall Attack Rates**

263 We then projected how the overall attack rates among the residents of the
264 metropolitan area of Barcelona would change at different levels of physical
265 distancing. We began the simulations with daily social contacts equaled to 100%
266 of baseline (i.e., no physical distancing) and gradually reduced them to 20% of
267 baseline. The simulations were performed with or without contact tracing, using
268 three different R_0 as aforementioned (Figure 5).

269 With the original Wuhan SARS-CoV-2 strain, if there were no physical
270 distancing measures in place (100% of baseline social contacts) and the diagnosis
271 relied on only passive surveillance (no contact tracing), we predicted that 78.7% of
272 the population in Barcelona would be infected (95% credible interval, 66.0-86.8%).
273 With contact tracing, the proportion of infected decreased to 60.0% of the overall

274 population (95% credible interval, 36.1-77.0%). In both scenarios (with and without
275 contact tracing), with the strengthening of physical distancing, the predicted
276 attack rates would also decrease simultaneously (Figure 5). When compared to the
277 scenarios without contact tracing, the predicted attack rates were constantly lower
278 in scenarios with contact tracing systems in place. We believed that these results
279 demonstrated the synergistic effect of these two prevention measures, and that
280 contact tracing would remain a valuable adjunctive measure despite the decline in
281 detection probabilities related to physical distancing.

282 If we aimed to keep the overall attack rate under 5% of the total population
283 during the model simulation, it required a 50% (95% credible interval, 39-69%)
284 reduction of daily social contacts when a contact tracing system was not
285 functioning, as compared to a much lower target of 36% (95% credible interval,
286 22-50% reduction) when contact tracing is implemented. The thresholds for
287 keeping overall attack rates under 2% of total populations were 56% (95% credible
288 interval, 45-62%) and 43% (95% credible interval, 31-46%) reductions of baseline
289 social contacts, without or with contact tracing, respectively (Table 3).

290

291 **3.3. Predicted Attack Rates with Different Basic Reproduction Number**

292 We observed similar results with the other two strains in our simulation
293 (Figure 5). For VOC B.1.1.7, without physical distancing, we predicted that 75.9%
294 (95% credible interval, 62.3-84.2%) and 87.3% of the population (95% credible
295 interval, 80.9-92.6%) would be infected, with and without contact tracing,
296 respectively. As for VOC B.1.167.2, when physical distancing was not implemented,
297 the median predicted infected proportion of the population was 90.3% (95%
298 credible interval, 84.9-93.6%) and 95.8% (95% credible interval, 93.3-97.5%), with
299 and without contact tracing, respectively.

300 With both variants, the strengthening of physical distancing resulted in a
301 decrease in the estimated population infected in the model (Figure 5). In the
302 scenarios with both variants, despite the interaction between physical distancing
303 and contact tracing system, implementing contact tracing remained an effective
304 supplement to physical distancing and could further reduced the population
305 infection by COVID-19 in the model. The levels of physical distancing required to
306 control the epidemics are listed in Table 3.

307

308 **4. Discussion**

309 In this study, we have developed a modeling framework to estimate the
310 detection probability of SARS-CoV-2 infection with different surveillance strategies
311 (passive surveillance with and without active contact tracing). The estimations
312 were then used to simulate the overall attack rates with different levels of physical
313 distancing. We demonstrated how the probability of COVID-19 detection interacts
314 with the physical distancing measures. According to our model, the effectiveness
315 of contact tracing may decrease due to the strengthening of physical distancing
316 measures, but it will remain an effective supplementary approach in controlling
317 epidemics.

318 Like our study, many researchers have attempted to estimate the effectiveness
319 of contact tracing as part of COVID-19 surveillance and control (Kretzschmar et al.,
320 2020; Quilty et al., 2021; Stuart et al., 2021; Vecino-Ortiz, Congote, Bedoya, &
321 Cucunuba, 2021; Willem et al., 2021). Hypothetic scenarios have been proposed
322 and simulated to assess the potential impacts of active contact tracing
323 deployment. However, some of these scenarios might be difficult to accomplish in
324 real life (e.g., 100% adherence to quarantine, 100% testing of contacts, etc.). In our
325 study, we attempted to quantify the real-life detection probability achieved with
326 the Spanish algorithm of diagnosis and screening (Ministerio de Sanidad España,

327 2020). Furthermore, most of these models did not consider how physical
328 distancing might impact the performance of contact tracing operational systems
329 (Kretzschmar et al., 2020; Quilty et al., 2021; Vecino-Ortiz et al., 2021). Therefore,
330 we attempted to develop a tool to estimate the interaction between physical
331 distancing measures and contact tracing. Our modeling framework is also quite
332 flexible and can be adapted to fit variables of different healthcare systems or other
333 populations, allowing to compare the effect of similar interventions on different
334 settings.

335 With the scenario tree analysis, we estimated that the COVID-19 detection
336 probabilities in Catalonia ranged from 8.0% to 36.5% across different age strata if
337 the diagnosis relied solely on passive surveillance. The low detection probability
338 was consistent with the findings of large seroprevalence studies conducted during
339 the first wave of COVID-19 epidemics around the world, when most public health
340 authorities were struggling to trace infected cases (Byambasuren et al., 2021;
341 Grant et al., 2021; Pollán et al., 2020). In Spain, the comparison between reported
342 cases and the seroprevalence in the ENE-COVID study suggested that only 10% of
343 cases were reported by May 2020 (Pollán et al., 2020). The estimates were 12%
344 and 29% in Belgium and Luxembourg, respectively (Grant et al., 2021).

345 Assuming the contact tracing system to be fully operational, we estimated
346 that the detection probabilities of the original Wuhan strain ranged from 46.7% to
347 66.5% without physical distancing measures. In our model, the detection
348 probability of COVID-19 would decrease gradually as we strengthened the
349 physical distancing measures and the circulation of viruses was reduced in the
350 population (Figure 4). This reduction was strongly associated with the reduction in
351 the average numbers of infected contacts. In our estimates, the detection
352 probabilities with extreme physical distancing (with only a 20% baseline of daily
353 social contacts allowed) were 15.8% to 43.2%. Despite the reduced detection
354 probability caused by the interaction with physical distancing, contact tracing
355 remained an effective supplementary approach to reducing overall attack rates
356 and epidemics (Figure 5). Similar results were also demonstrated in the simulation
357 of different strains with higher R_0 .

358 In general, prolonged and extreme population-wide lockdowns are often
359 impractical due to their negative socioeconomic impact (Gopinath, 2020).
360 Furthermore, recent studies suggest that prolonged lockdowns might also result
361 in long-term medical problems (López-Bueno et al., 2021; Singh et al., 2020). In
362 our model, we demonstrated that contact tracing could serve as an adjunctive
363 measure to exert similar control of epidemics with a less strict level of physical

364 distancing measures. The requirement of social contacts minimization could be
365 reduced in the presence of contact tracing systems as compared with physical
366 distancing alone (Table 3). Similar to our findings, the synergistic effect of these
367 two control measures was also proposed by other researchers. For example,
368 experience during early epidemics in Taiwan and South Korea demonstrated the
369 combination of case-based (testing and contact tracing) and population-based
370 (social distancing) interventions was important for the early containment of
371 COVID-19 before vaccination was available (Chen & Fang, 2021; Chen, Fang, &
372 Huang, 2021; Ng et al., 2021).

373 Our study had several limitations and should be interpreted with caution. In
374 the model, we assumed the average compliance to quarantine procedures was
375 50%. To our knowledge, some countries have implemented various measures to
376 ensure the compliance of quarantine and the impact of contact tracing might
377 increase accordingly with these policies (Ministry of Health and Welfare Taiwan,
378 2020). Moreover, even in the same healthcare system, compliance could change
379 significantly in different areas or different subpopulations. The capacity of contact
380 tracing by public health authorities might also be heavily impacted by the number
381 of infected cases, which was not considered in our model. Furthermore, estimating
382 the effectiveness of physical distancing is also important when applying our

383 model. Although a drastic reduction of 80% (from 100% to 20%) in the baseline
384 daily contacts was proposed in our study, it might be very difficult to accomplish
385 in real life. In Spain, after the relaxation of nationwide lockdown in May 2020, the
386 number of daily contacts grew rapidly in the area of Barcelona, despite some
387 mobility restrictions being still instated, and the reduction in daily contacts was
388 estimated to be only around 25%.

389 Furthermore, the time required for establishing a diagnosis was also
390 important for the control of epidemics. Early diagnosis would lead to early
391 isolation of infected individuals and greater reduction of transmission. In our
392 study, the rates of detection were calculated by the probability-rate equation
393 describing the transition between two states (Gidwani & Russell, 2020). In reality,
394 the rate depends largely on the efficiency of the public health service and may
395 vary significantly in different settings. In a study evaluating the contact tracing
396 procedure in the United States, it could take up to more than 10 days to notify the
397 exposed contacts (Lash et al., 2021). Therefore, it is also important for
398 policymakers to monitor the performance of contact tracing system and
399 implement different methodologies to improve its efficiency (Garry, Hope, Zajac,
400 Verrall, & Robertson, 2021). For example, a study in the United Kingdom has

401 demonstrated the correlation between the uptake of the NHS smartphone app
402 and the reduction of local COVID-19 cases (Wymant et al., 2021).

403 One of the main limitations of our model is that our ST analyses were
404 deterministic. Considering the high complexity of the contact tracing system in
405 real life and its interaction with the contact matrices, it is very likely that a certain
406 amount of randomness should be taken into account during calculation.
407 Therefore, the point estimates of the detection probability obtained in this study
408 should be interpreted with great caution. However, since we had included a
409 stochastic factor during the calculation of the force of infection (λ) in the SEIR
410 model, we believed the final simulations had included adequate stochastic
411 variations to represent the possible outcomes in real life.

412 We made several simplifications during the construction and
413 parameterization of the model. Firstly, in order to reduce the complexity, we only
414 considered the general public in the metropolitan area of Barcelona, and the
415 residents in the long-term care facilities were not included. The model was applied
416 to a closed population and the movement of population was not considered. The
417 coverage of vaccination, healthcare-related infections, and the possibility of re-
418 infection were neither featured in the model. These factors could largely change
419 the magnitude of COVID-19 epidemics. Furthermore, we did not consider the

420 potential false positives of the diagnostic tests since they do not contribute to the
421 transmission of viruses. We also assumed all fatal cases would be admitted to an
422 ICU before death. This assumption is designed to gauge the maximal requirement
423 of ICU beds. Therefore, caution must be taken when comparing our simulations in
424 this study to real-life reports. Due to these simplifications and aforementioned
425 limitations, we were unable to validate our model outputs with real-life
426 observations in the study. The rapid change of our understanding of COVID-19
427 and local disease containment policies during the epidemics has also increased
428 the difficulty of validation. However, since these factors had little interaction with
429 physical distancing measures and the diagnosis system, we believed that the
430 comparisons between different physical distancing and surveillance strategies in
431 our modeling framework are still informative. Moreover, if necessary, the
432 framework can also be easily modified to accommodate new variables and
433 provide viable simulations of real-life scenarios.

434 In our study, we assumed that daily social contacts would decrease
435 homogeneously across different age strata. However, it is possible that different
436 policies implemented in real life would affect different populations. Therefore, we
437 also simulated several scenarios with physical distancing policies focusing on
438 different age strata, and the conclusion was similar to current findings (data not

439 shown). Nevertheless, decision-makers should consider how the effects of physical
440 distancing policies might affect different populations (ages, sectors, genders)
441 before applying our results.

442 In terms of surveillance, several key parameters we used in the calculation
443 required validation when applied in different healthcare systems. These
444 parameters might change significantly with different public health policies and
445 infrastructure. We believe that our calculation provides a possible means to
446 estimate the overall detection probability, but the variables used during the
447 calculation need to be tailored accordingly in different healthcare systems.

448 In conclusion, we developed a model combining ST analysis and a SEIR
449 compartmental model, which can be used to assess the impact of surveillance
450 strategies and their interactions with physical distancing. In our simulation, the
451 detection probability of COVID-19 with a contact tracing system would decrease
452 gradually as we strengthened physical distancing measures. However, contact
453 tracing would remain a valuable adjunctive measure to mitigate the impact of
454 COVID-19 epidemics.

455

456 Acknowledgements

457 This research is part of the Master's Dissertation by Guan-Jhou Chen for the

458 Erasmus Mundus Joint Master's Degree in Infectious Disease and One Health

459 (<https://www.infectious-diseases-one-health.eu/>).

460 Our thanks to Professor Javier Sanchez of the Atlantic Veterinary College of Prince

461 Edward Island, Canada for his assistance and input during the conceptualization

462 of this study. To Professor Ashleigh R. Tuite of the University of Toronto for her

463 advice on the data analysis and model building. To Ermengol Coma i Redon and

464 Manuel Medina Peralta of the SISAP, ICS for providing demographic and

465 reporting data of Catalonia.

466

467 Funding

468 F.B. and J.R.B.P. acknowledge funding from the European Commission, under
469 Grants 874735 (VEO), 853271 (H-MIP), and 2020/2094 (NextGenerationEU,
470 through CSIC's Global Health Platform, PTI Salud Global).

471

472 Author contributions

473 G-J. C participated in the conceptualization, software adaptation and design,
474 analysis, and interpretation of the study's data, as well as the writing of the original
475 publication. JP and FB contributed to the analysis and interpretation of data related
476 to contact matrix and social distance, reviewing and editing. AA was in charge of
477 supervision and design of the study; data curation and analysis and interpretation;
478 and reviewing and editing of intellectual content. All authors had full access to all
479 the data in the study and accepted responsibility for submitting it for publication.

480

481 Conflict of interest

482 All authors declare that no conflicts of interest exist.

483

484 **References**

485 Anderson, R. M., Heesterbeek, H., Klinkenberg, D., & Hollingsworth, T. D. (2020).

486 How will country-based mitigation measures influence the course of the

487 COVID-19 epidemic? *The Lancet*, *395*(10228), 931–934.

488 [https://doi.org/10.1016/S0140-6736\(20\)30567-5](https://doi.org/10.1016/S0140-6736(20)30567-5)

489 Brisson, M., Drolet, M., Mondor, M., Godbout, A., Gingras, G., Demers, E., & Institut

490 national de santé publique du Québec. (2021). CONNECT: étude des contacts

491 sociaux des Québécois. Retrieved February 5, 2021, URL

492 <https://www.inspq.qc.ca/covid-19/donnees/connect/29-janvier-2021>

493 Byambasuren, O., Dobler, C. C., Bell, K., Rojas, D. P., Clark, J., McLaws, M. L., &

494 Glasziou, P. (2021). Comparison of seroprevalence of SARS-CoV-2 infections

495 with cumulative and imputed COVID-19 cases: Systematic review. *PLoS ONE*,

496 *16*(4), e0248946. <https://doi.org/10.1371/journal.pone.0248946>

497 Chen, Y.-H., & Fang, C.-T. (2021, February). Combined interventions to suppress R0

498 and border quarantine to contain COVID-19 in Taiwan. *Journal of the*

499 *Formosan Medical Association*. <https://doi.org/10.1016/j.jfma.2020.08.003>

500 Chen, Y.-H., Fang, C.-T., & Huang, Y.-L. (2021). Effect of Non-lockdown Social

501 Distancing and Testing-Contact Tracing During a COVID-19 Outbreak in

502 Daegu, South Korea, February to April 2020: A Modeling Study. *International*

- 503 *Journal of Infectious Diseases*, 110, 213–221.
- 504 <https://doi.org/10.1016/j.ijid.2021.07.058>
- 505 Chu, D. K., Akl, E. A., Duda, S., Solo, K., Yaacoub, S., Schünemann, H. J., ... Reinap,
506 M. (2020). Physical distancing, face masks, and eye protection to prevent
507 person-to-person transmission of SARS-CoV-2 and COVID-19: a systematic
508 review and meta-analysis. *The Lancet*, 395(10242), 1973–1987.
- 509 [https://doi.org/10.1016/S0140-6736\(20\)31142-9](https://doi.org/10.1016/S0140-6736(20)31142-9)
- 510 Food and Agriculture Organization (FAO). (2014). *Risk-based disease surveillance*
511 *- a manual for veterinarians on the design and analysis of surveillance for*
512 *demonstration of freedom from disease*. Rome.
- 513 Garry, M., Hope, L., Zajac, R., Verrall, A. J., & Robertson, J. M. (2021). Contact
514 Tracing: A Memory Task With Consequences for Public Health. *Perspectives*
515 *on Psychological Science*, 16(1), 175–187.
- 516 <https://doi.org/10.1177/1745691620978205>
- 517 Gidwani, R., & Russell, L. B. (2020). Estimating Transition Probabilities from
518 Published Evidence: A Tutorial for Decision Modelers. *PharmacoEconomics*,
519 38(11), 1153–1164. <https://doi.org/10.1007/s40273-020-00937-z>
- 520 Girum, T., Lentiro, K., Geremew, M., Migora, B., & Shewamare, S. (2020). Global
521 strategies and effectiveness for COVID-19 prevention through contact tracing,

- 522 screening, quarantine, and isolation: a systematic review. *Tropical Medicine*
523 *and Health*, 48(1), 91. <https://doi.org/10.1186/s41182-020-00285-w>
- 524 Gopinath, G. (2020). The Great Lockdown: Worst Economic Downturn Since the
525 Great Depression – IMF Blog. Retrieved July 2, 2021, URL
526 [https://blogs.imf.org/2020/04/14/the-great-lockdown-worst-economic-](https://blogs.imf.org/2020/04/14/the-great-lockdown-worst-economic-downturn-since-the-great-depression/)
527 [downturn-since-the-great-depression/](https://blogs.imf.org/2020/04/14/the-great-lockdown-worst-economic-downturn-since-the-great-depression/)
- 528 Grant, R., Dub, T., Andrianou, X., Nohynek, H., Wilder-Smith, A., Pezzotti, P., &
529 Fontanet, A. (2021). SARS-CoV-2 population-based seroprevalence studies in
530 Europe: A scoping review. *BMJ Open*, 11(4), e045425.
531 <https://doi.org/10.1136/bmjopen-2020-045425>
- 532 Guan, W., Ni, Z., Hu, Y., Liang, W., Ou, C., He, J., ... Zhong, N. (2020). Clinical
533 Characteristics of Coronavirus Disease 2019 in China. *New England Journal of*
534 *Medicine*, 382(18), 1708–1720. <https://doi.org/10.1056/nejmoa2002032>
- 535 Kortela, E., Kirjavainen, V., Ahava, M. J., Jokiranta, S. T., But, A., Lindahl, A.,
536 Jääskeläinen, A.E., Jääskeläinen, A.J., Järvinen, A., Jokela, P., Kallio-Kokko, H.,
537 Loginov, R., Mannonen, L., Ruotsalainen, E., Sironen, T., Vapalahti, O.,
538 Lappalainen, M., Kreivi, H.-R., Jarva, H., Kurkela, S., Kekäläinen, E. (2021). Real-
539 life clinical sensitivity of SARS-CoV-2 RT-PCR test in symptomatic patients.
540 *PLoS ONE*, 16(5), e0251661. <https://doi.org/10.1371/journal.pone.0251661>

- 541 Kretzschmar, M. E., Rozhnova, G., Bootsma, M. C. J., van Boven, M., van de Wijgert,
542 J. H. H. M., & Bonten, M. J. M. (2020). Impact of delays on effectiveness of
543 contact tracing strategies for COVID-19: a modelling study. *The Lancet Public
544 Health*, 5(8), e452–e459. [https://doi.org/10.1016/S2468-2667\(20\)30157-2](https://doi.org/10.1016/S2468-2667(20)30157-2)
- 545 Kucharski, A. J., Klepac, P., Conlan, A. J. K., Kissler, S. M., Tang, M. L., Fry, H., Gog,
546 J.R., Edmunds, W.J., CMMID COVID-19 working group. (2020). Effectiveness of
547 isolation, testing, contact tracing, and physical distancing on reducing
548 transmission of SARS-CoV-2 in different settings: a mathematical modelling
549 study. *The Lancet Infectious Diseases*, 20(10), 1151–1160.
550 [https://doi.org/10.1016/S1473-3099\(20\)30457-6](https://doi.org/10.1016/S1473-3099(20)30457-6)
- 551 Lash, R. R., Moonan, P. K., Byers, B. L., Bonacci, R. A., Bonner, K. E., Donahue, M.,
552 Donovan, C.V., Grome, H.N., Janssen, J.M., Magleby, R., McLaughlin, H.P.,
553 Miller, J.S., Pratt, C.Q., Steinberg, J., Varela, K., Anschuetz, G.L., Cieslak, P.R.,
554 Fialkowski, V., Fleischauer, A.T., Goddard, C., Johnson, S.J., Morris, M., Moses,
555 J., Newman, A., Prinzing, L., Sulka, A.C., Va, P., Willis, M., Oeltmann, J.E.,
556 COVID-19 Contact Tracing Assessment Team. (2021). COVID-19 Case
557 Investigation and Contact Tracing in the US, 2020. *JAMA Network Open*, 4(6),
558 1–12. <https://doi.org/10.1001/jamanetworkopen.2021.15850>
- 559 López-Bueno, R., López-Sánchez, G. F., Casajús, J. A., Calatayud, J., Tully, M. A., &

- 560 Smith, L. (2021). Potential health-related behaviors for pre-school and school-
561 aged children during COVID-19 lockdown: A narrative review. *Preventive*
562 *Medicine, 143*, 106349. <https://doi.org/10.1016/j.jpmed.2020.106349>
- 563 Ministerio de Sanidad España. (2020). Estrategia de Detección Precoz, Vigilancia y
564 Control de COVID-19. Retrieved July 1, 2021, URL
565 <https://www.mscbs.gob.es/profesionales/saludPublica/ccayes/alertasActual/n>
566 [Cov/documentos/COVID19 Estrategia vigilancia y control e indicadores.pdf](https://www.mscbs.gob.es/profesionales/saludPublica/ccayes/alertasActual/nCov/documentos/COVID19_Estrategia_vigilancia_y_control_e_indicadores.pdf)
- 567 Ministry of Health and Welfare Taiwan. (2020). Combined the "Entry Quarantine
568 System" and "Digital Fencing Tracking System" and utilize mobile positioning
569 to monitor movement of individuals. Retrieved July 1, 2021, URL
570 <https://covid19.mohw.gov.tw/en/cp-4868-53887-206.html>
- 571 Mossong, J., Hens, N., Jit, M., Beutels, P., Auranen, K., Mikolajczyk, R., Massari, M.,
572 Salmaso, S., Tomba, G.S., Wallinga, J., Heijne, J., Sadkowska-Todys, M.,
573 Rosinska, M., Edmunds, W. J. (2008). Social contacts and mixing patterns
574 relevant to the spread of infectious diseases. *PLoS Medicine, 5*(3), e74.
575 <https://doi.org/10.1371/journal.pmed.0050074>
- 576 Ng, T. C., Cheng, H. Y., Chang, H. H., Liu, C. C., Yang, C. C., Jian, S. W., Liu, D.P.,
577 Cohen, T., Lin, H. H. (2021). Comparison of Estimated Effectiveness of Case-
578 Based and Population-Based Interventions on COVID-19 Containment in

- 579 Taiwan. *JAMA Internal Medicine*, 181(7), 913–921.
- 580 <https://doi.org/10.1001/jamainternmed.2021.1644>
- 581 WHO. (2021). Considerations in adjusting public health and social measures in the
582 context of COVID-19. *World Health Organisation Interim Guidance*,
583 (November), 1–13. URL
584 [https://www.who.int/publications/i/item/considerations-in-adjusting-public-](https://www.who.int/publications/i/item/considerations-in-adjusting-public-health-and-social-measures-in-the-context-of-covid-19-interim-guidance)
585 [health-and-social-measures-in-the-context-of-covid-19-interim-guidance](https://www.who.int/publications/i/item/considerations-in-adjusting-public-health-and-social-measures-in-the-context-of-covid-19-interim-guidance)
- 586 Palmer, J., Ottow, R., & Bartumeus, F. (2021). DISTANCIA-COVID: Impacto de las
587 medidas de distanciamiento social sobre la expansión de la epidemia de
588 COVID-19 en España. Retrieved June 16, 2021, URL [https://distancia-](https://distancia-covid.csic.es/)
589 [covid.csic.es/](https://distancia-covid.csic.es/)
- 590 Pollán, M., Pérez-Gómez, B., Pastor-Barriuso, R., Oteo, J., Hernán, M. A., Pérez-
591 Olmeda, M., Sanmartín, J.L., Fernández-García, A., Cruz, I., de Larrea, N.F.,
592 Molina, M., Rodríguez-Cabrera, F., Martín, M., Merino-Amador, P., Paniagua,
593 J.L., Muñoz-Montalvo, J.F., Blanco, F., Yotti, R., ENE-COVID Study Group.
594 (2020). Prevalence of SARS-CoV-2 in Spain (ENE-COVID): a nationwide,
595 population-based seroepidemiological study. *The Lancet*, 396(10250), 535–
596 544. [https://doi.org/10.1016/S0140-6736\(20\)31483-5](https://doi.org/10.1016/S0140-6736(20)31483-5)
- 597 Quilty, B. J., Clifford, S., Hellewell, J., Russell, T. W., Kucharski, A. J., Flasche, S., ,

- 598 Edmunds, W.J., Centre for the Mathematical Modelling of Infectious Diseases
599 COVID-19 working group. (2021). Quarantine and testing strategies in contact
600 tracing for SARS-CoV-2: a modelling study. *The Lancet Public Health*, 6(3),
601 e175–e183. [https://doi.org/10.1016/S2468-2667\(20\)30308-X](https://doi.org/10.1016/S2468-2667(20)30308-X)
- 602 Redondo-Bravo, L., Moros, M. J. S., Sanchez, E. V. M., Lorusso, N., Ubago, A. C.,
603 Garcia, V. G., Working group for the surveillance and control of COVID-19 in
604 Spain. (2020). The first wave of the COVID-19 pandemic in Spain:
605 Characterisation of cases and risk factors for severe outcomes, as at 27 April
606 2020. *Eurosurveillance*, 25(50), 2001431. [https://doi.org/10.2807/1560-](https://doi.org/10.2807/1560-7917.ES.2020.25.50.2001431)
607 [7917.ES.2020.25.50.2001431](https://doi.org/10.2807/1560-7917.ES.2020.25.50.2001431)
- 608 Saurabh, S., & Prateek, S. (2017). Role of contact tracing in containing the 2014
609 Ebola outbreak: A review. *African Health Sciences*, 17(1), 225–236.
610 <https://doi.org/10.4314/ahs.v17i1.28>
- 611 Singh, S., Roy, D., Sinha, K., Parveen, S., Sharma, G., & Joshi, G. (2020). Impact of
612 COVID-19 and lockdown on mental health of children and adolescents: A
613 narrative review with recommendations. *Psychiatry Research*, 293, 113429.
614 <https://doi.org/10.1016/j.psychres.2020.113429>
- 615 Soetaert, K., Petzoldt, T., & Setzer, R. W. (2010). Solving differential equations in R:
616 Package deSolve. *Journal of Statistical Software*, 33(9), 1–25.

- 617 <https://doi.org/10.18637/jss.v033.i09>
- 618 Stuart, R. M., Abey Suriya, R. G., Kerr, C. C., Mistry, D., Klein, D. J., Gray, R. T., ... Scott,
619 N. (2021). Role of masks, testing and contact tracing in preventing COVID-19
620 resurgences: A case study from New South Wales, Australia. *BMJ Open*, *11*(4),
621 1–10. <https://doi.org/10.1136/bmjopen-2020-045941>
- 622 Szabados, T. (2010). An elementary introduction to the Wiener process and
623 stochastic integrals. *Studia Scientiarum Mathematicarum Hungarica*, *31*.
- 624 Thakur, B., Dubey, P., Benitez, J., Torres, J. P., Reddy, S., Shokar, N., Aung, K.,
625 Mukherjee, D., Dwivedi, A. K. (2021). A systematic review and meta-analysis of
626 geographic differences in comorbidities and associated severity and mortality
627 among individuals with COVID-19. *Scientific Reports*, *11*(1), 8562.
628 <https://doi.org/10.1038/s41598-021-88130-w>
- 629 Tuite, A. R., Fisman, D. N., & Greer, A. L. (2020). Mathematical modelling of COVID-
630 19 transmission and mitigation strategies in the population of Ontario,
631 Canada. *Canadian Medical Association Journal*, *192*(19), e497–e505.
632 <https://doi.org/10.1503/cmaj.200476>
- 633 Vecino-Ortiz, A. I., Congote, J. V., Bedoya, S. Z., & Cucunuba, Z. M. (2021). Impact
634 of contact tracing on COVID-19 mortality: An impact evaluation using
635 surveillance data from Colombia. *PLoS ONE*, *16*(3), e0246987.

- 636 <https://doi.org/10.1371/journal.pone.0246987>
- 637 Wang, D., Hu, B., Hu, C., Zhu, F., Liu, X., Zhang, J., Wang, B., Xiang, H., Cheng, Z.,
638 Xiong, Y., Zhao, Y., Li, Y., Wang, X., Peng, Z. (2020). Clinical Characteristics of
639 138 Hospitalized Patients With 2019 Novel Coronavirus-Infected Pneumonia
640 in Wuhan, China. *JAMA*, *323*(11), 1061–1069.
641 <https://doi.org/10.1001/jama.2020.1585>
- 642 Willem, L., Abrams, S., Libin, P. J. K., Coletti, P., Kuylen, E., Petrof, O., Møgelmoose, S.,
643 Wambua, J., Herzog, S.A., Faes, C., Beutels, P., Hens, N. (2021). The impact of
644 contact tracing and household bubbles on deconfinement strategies for
645 COVID-19. *Nature Communications*, *12*(1), 1–9.
646 <https://doi.org/10.1038/s41467-021-21747-7>
- 647 Woloshin, S., Patel, N., & Kesselheim, A. S. (2020). False Negative Tests for SARS-
648 CoV-2 Infection — Challenges and Implications. *New England Journal of*
649 *Medicine*, *383*(6), e38. <https://doi.org/10.1056/nejmp2015897>
- 650 Wymant, C., Ferretti, L., Tsallis, D., Charalambides, M., Abeler-Dörner, L., Bonsall, D.,
651 Hinch, R., Kendall, M., Milsom, L., Ayres, M., Holmes, C., Briers, M., Fraser, C.
652 (2021). The epidemiological impact of the NHS COVID-19 app. *Nature*,
653 *594*(7863), 408–412. <https://doi.org/10.1038/s41586-021-03606-z>
- 654 Yang, X., Yu, Y., Xu, J., Shu, H., Xia, J., Liu, H., Wu, Y., Zhang, L., Yu, Z., Fang, M., Yu,

- 655 T., Wang, T., Pan, S., Zou, X., Yuan, S., Shang, Y. (2020). Clinical course and
656 outcomes of critically ill patients with SARS-CoV-2 pneumonia in Wuhan,
657 China: a single-centered, retrospective, observational study. *The Lancet*
658 *Respiratory Medicine*, 8(5), 475–481. [https://doi.org/10.1016/S2213-](https://doi.org/10.1016/S2213-2600(20)30079-5)
659 [2600\(20\)30079-5](https://doi.org/10.1016/S2213-2600(20)30079-5)
- 660 Zhu, N., Zhang, D., Wang, W., Li, X., Yang, B., Song, J., Zhao, X., Huang, B., Shi, W.,
661 Lu, R., Niu, P., Zhan, F., Ma, X., Wang, D., Xu, W., Wu, G., Gao, G.F., Tan W.,
662 China Novel Coronavirus Investigating and Research Team. (2020). A Novel
663 Coronavirus from Patients with Pneumonia in China, 2019. *New England*
664 *Journal of Medicine*, 382(8), 727–733. <https://doi.org/10.1056/nejmoa2001017>
- 665

666 **Table 1.** Parameters of the scenario tree analyses for the passive surveillance and contact
 667 tracing system.

Parameter	Age	Value	Description & Reference
<i>Passive surveillance (see Figure 3)</i>			
<i>p. symptom_i</i>	0-14	0.2	Probability of presenting clinical symptoms after being infected by SARS-CoV-2 in each age stratum.
	15-49	0.4	
	50-64	0.5	
	≥65	0.6	
<i>p. healthcare_i</i>	0-14	0.6	Probabilities of an individual seeking medical attention or consulting a healthcare service after developing clinical symptoms. The default values were assumed based on past experience and may vary significantly depending on the availability of the healthcare system.
	15-49	0.6	
	50-64	0.7	
	≥65	0.8	
<i>p. test. pass_i</i>	0-14	0.7	Probabilities of taking a COVID-19 diagnostic test after the consultation with a healthcare service. The default values were assumed based on past experience and may vary significantly depending on the availability of the healthcare system.
	15-49	0.7	
	50-64	0.8	
	≥65	0.8	
<i>se. symp</i>	All	0.95	Sensitivity of the diagnostic test for a symptomatic, SARS-CoV-2 infected patient. In Spain, patients with symptoms for less than 5 days would be tested by antigen-based tests and others by nucleic acid tests (Kortela et al., 2021; Ministerio de

Sanidad España, 2020; Woloshin, Patel, & Kesselheim, 2020).

$p. detect. pass_i$	0-14	0.080	Probabilities of positive cases being detected by passive surveillance (see Figure 5).
	15-49	0.160	Calculated as:
	50-64	0.266	$p. detect. pass_i = p. symptom_i \times p. healthcare_i \times p. test. pass_i \times se. symp$
	≥ 65	0.365	

Active surveillance (see Figure 4)

$p. cont. diag_i$	0-14		For primary cases in different age strata, this represents the probabilities of their
	15-49	variable [†]	infected contacts being diagnosed. The numbers were calculated with a baseline
	50-64		(pre-COVID) contact matrix and might change according to different contact
	≥ 65		matrices used in the calculation. See Supplement 1 for a detailed calculation.

$p. traceable_i$	0-14		Probabilities that at least one of the infected contacts was diagnosed, which would
	15-49		make the primary case traceable in the contact tracing system. Calculated as:
	50-64	variable [†]	$p. traceable_i = 1 - (1 - p. cont. diag_i)^n$
	≥ 65		The numbers were calculated with a baseline (pre-COVID) contact matrix and might change according to different contact matrices used in the calculation. See Supplement 1 for a detailed calculation.

n	All	$R0^{\dagger} + 1$	Average number of directly linked cases. Equals to the effective reproduction number (i.e. secondary cases) plus one (the source of the viruses).
-----	-----	--------------------	---

$p. test. act1_i$	0-14	0.70	Probabilities of a traceable case to be notified and tested for COVID-19. This variable
-------------------	------	------	---

15-49 0.70 accounted for the errors and incomppliance during contact tracing.

50-64 0.80

≥65 0.80

Sensitivity of the diagnostic test for infected close contacts of SARS-CoV-2,

se.contact

All 0.70

regardless of symptoms. In Spain, nucleic acid tests are required to confirm a close contact's being free of SARS-CoV-2 (Ministerio de Sanidad España, 2020).

0-14 0.9 Probabilities of taking a second COVID-19 diagnostic test due to the appearance of

15-49 0.9 clinical symptoms after an initial negative result. This variable accounts for the errors

p.test.act2_i

50-64 0.9 and incomppliance of the protocol.

≥65 0.9

Other parameters regarding the effectiveness of diagnosis and contact tracing

The average time from infection to detection of mild-to-moderate cases (days).

$1/\gamma_d$

All

variable

Calculated as:

$$\frac{1}{\gamma_d} = - \frac{\text{duration of infectiousness } (\gamma_m)}{\ln(1 - \text{detection probability})}$$

rr_i

All

0.5

Reduction of daily contacts frequency of individuals who were requested to be isolated or quarantined.

δ_e

All

variable

Probability of 'exposed' cases being identified and quarantined before becoming infectious. Calculated as:

$$\delta_e = \left(1 - e^{-\gamma_d \cdot 1/\varepsilon}\right) \times 0.8^8$$

†Calculated with different R0 and contact matrix, see Supplement 1 for detail.

‡See Supplement Table2 for details.

§Assuming there is a 20% loss or non-compliance during contact tracing.

668

Journal Pre-proof

669 **Table 2.** The baseline social contact matrix generated from the population-based
 670 contact diaries in eight European countries of the POLYMOD study

Age groups	Mean daily contact within each age stratum			
	0-14 years	15-49 years	50-64 years	≥ 65 years
0 - 14 years	6.28	3.71	0.55	0.24
15 - 49 years	1.77	11.60	1.60	0.28
50 - 64 years	1.34	6.52	2.57	0.52
≥ 65 years	0.89	2.97	1.34	1.55

671

672 **Table 3.** Estimating the required levels of physical distancing (% of reduction required for
 673 baseline daily social contacts) to keep the overall attack rates under designated
 674 thresholds in different scenarios.

Contact tracing system	Attack rate threshold <5%		Attack rate threshold <2%	
	No	Functioning	No	Functioning
With Original strain	50% (39-69%) [†]	36% (22-56%)	56% (45-52%)	43% (31-46%)
With VOC B.1.1.7	61% (53-68%)	48% (41-60%)	64% (58-71%)	56% (46-64%)
With VOC B.1.167.2	75% (70-80%)	68% (60-75%)	77% (73-81%)	71% (66-77%)

675 [†]The required reduction of daily social contacts for the given thresholds of attack
 676 rates. A higher percentage indicated a more strengthened and strict level of
 677 physical distancing.

678

679 **Figure Captions**

680 **Figure 1.** Illustration of the modelling framework combining scenario tree analyses and a
681 SEIR epidemiological model.

682

683 **Figure 2.** Scenario tree diagram representing the probability of detecting cases of COVID-
684 19 by passive surveillance. [†]The detection probability for each age stratum is calculated
685 separately.

686

687 **Figure 3.** Scenario tree diagram representing the probability of detecting positive cases
688 by contact tracing. [†]The detection probability for each age stratum is calculated
689 separately. [‡]According to the Spanish guidelines, contacts who were tested negative but
690 developed symptoms of COVID-19 would be managed and re-tested as suspected cases.

691

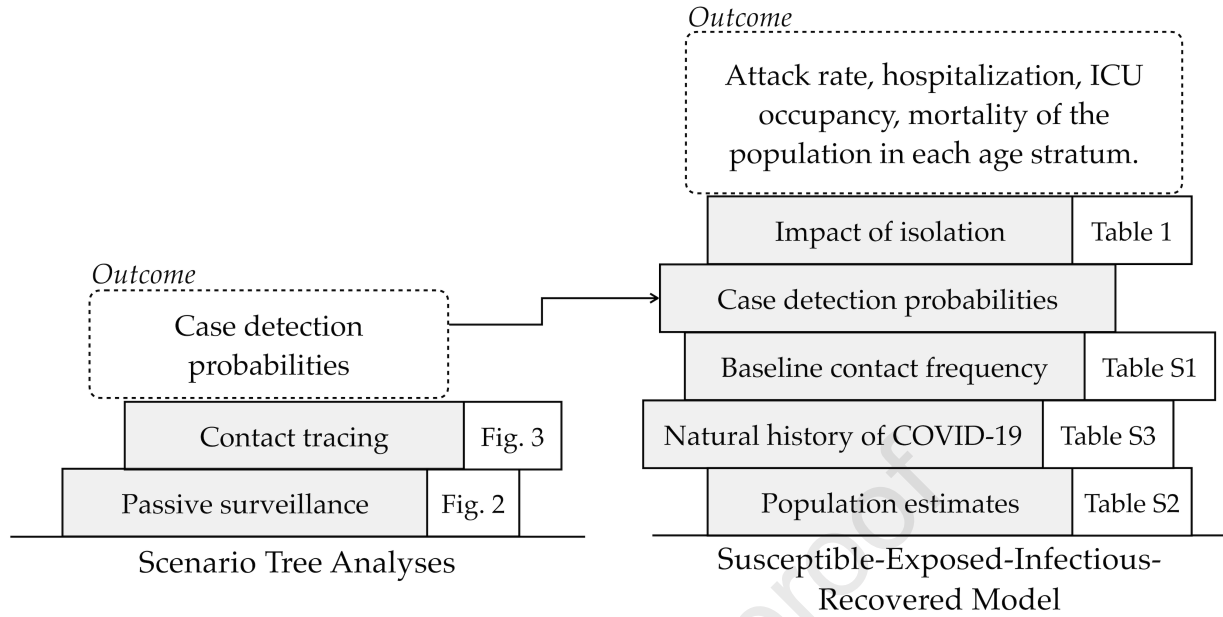
692 **Figure 4A, 4B, 4C.** The estimated probability of disease detection reduced with the
693 strengthening of physical distancing measures among different age strata with $R_0=2.6$ (A),
694 $R_0=3.4$ (B), and $R_0=5.1$ (C). The overall detection probabilities (p_{detect_i}) were
695 represented by solid lines. The detection probability with only passive surveillance
696 ($p_{detect.pass_i}$) were represented as dotted horizontal lines.

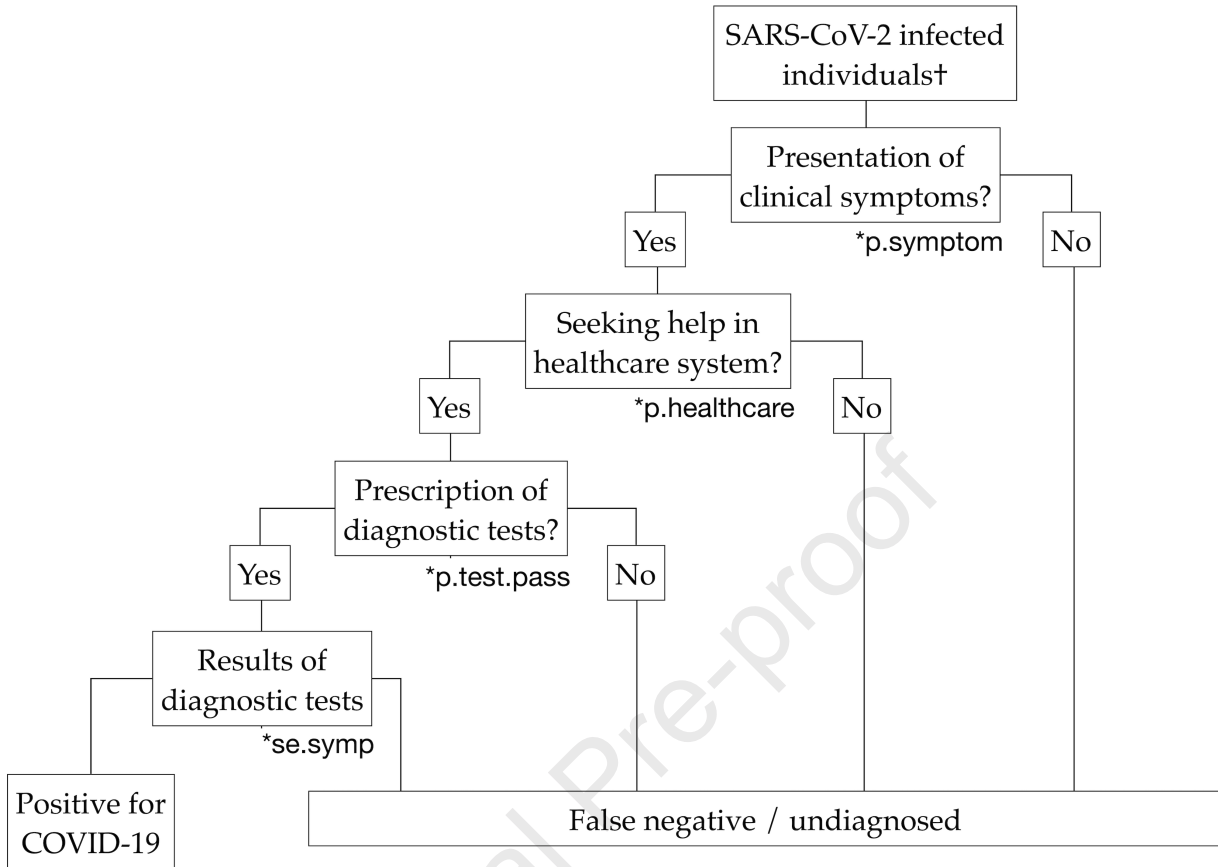
697

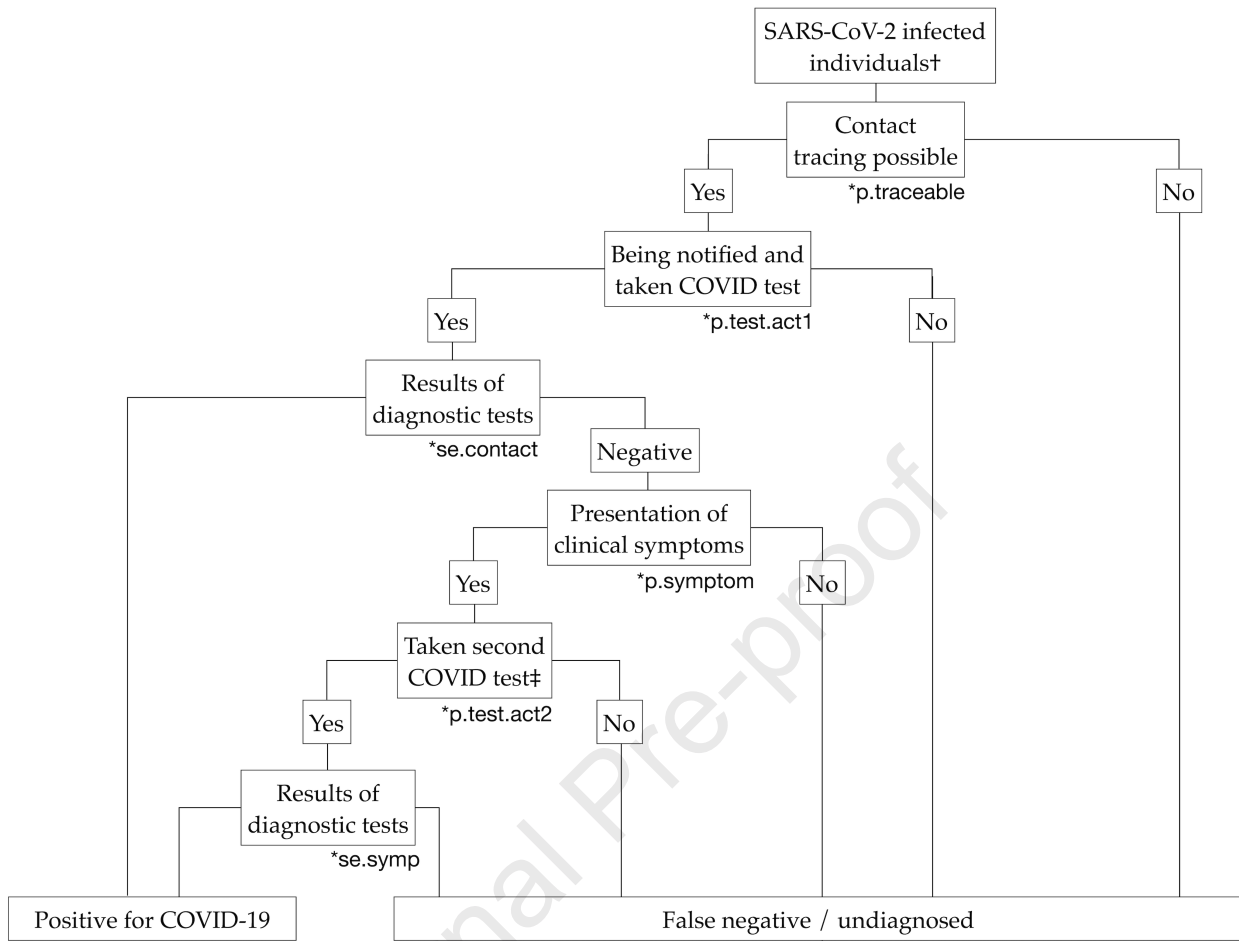
698

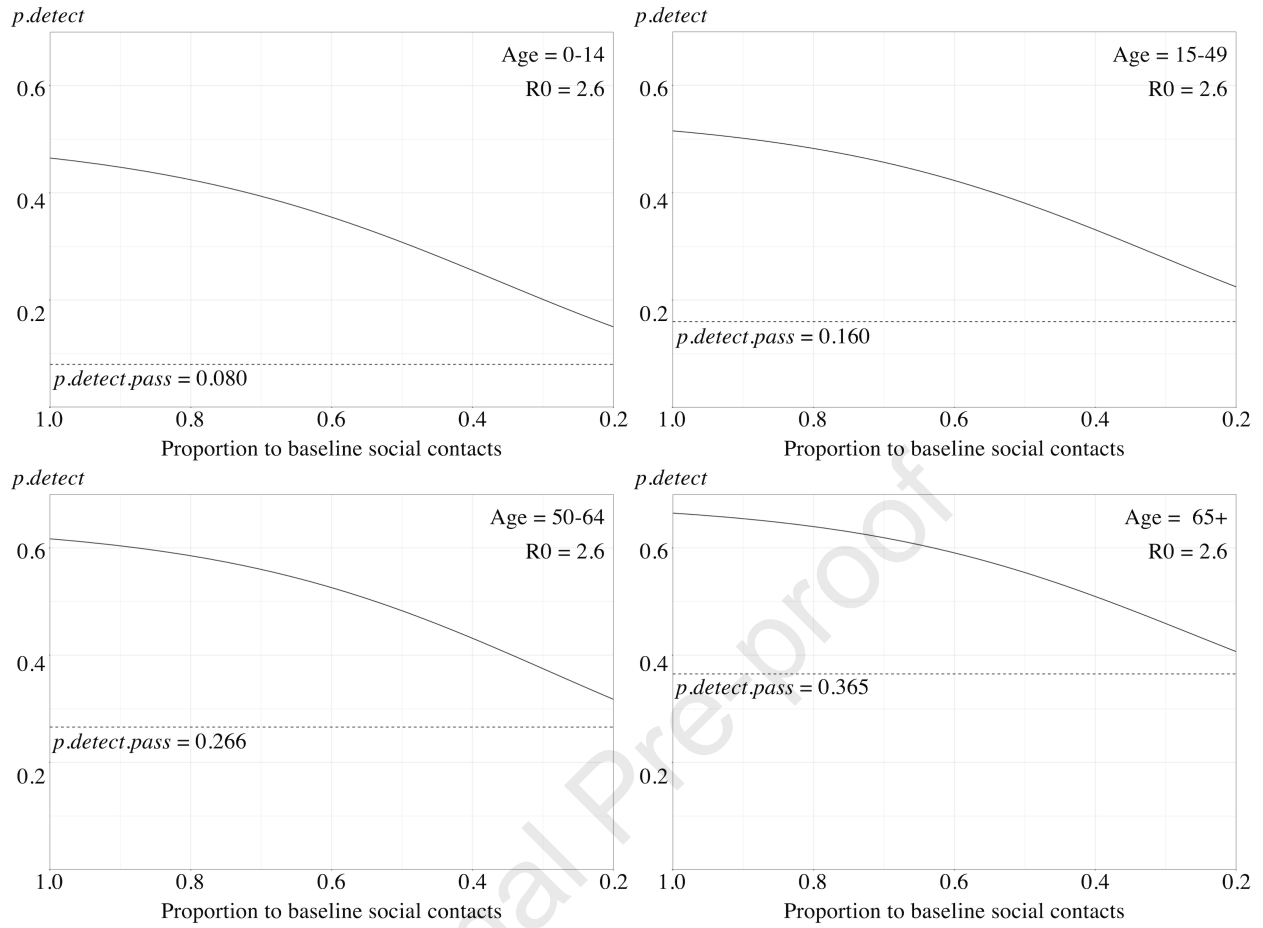
699 **Figure 5.** The predicted overall attack rates with different level of physical distancing
700 (represented by a reduced proportion of daily social contacts compared to a baseline) for
701 different basic reproduction number (R_0).
702

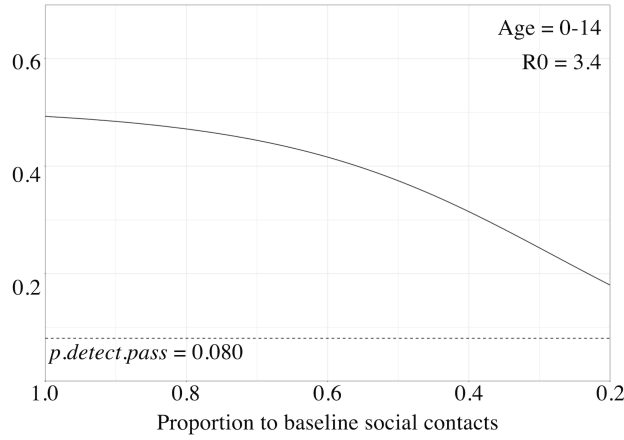
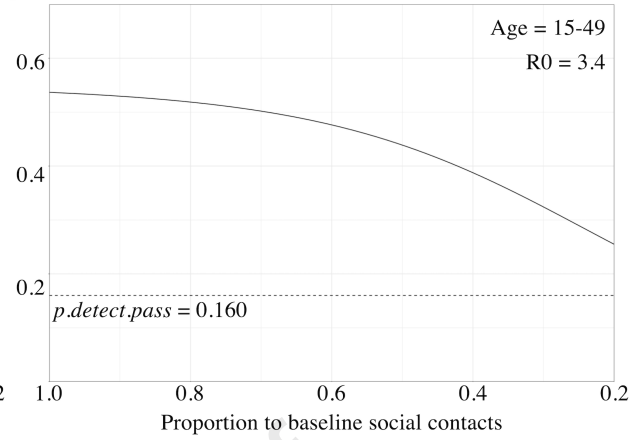
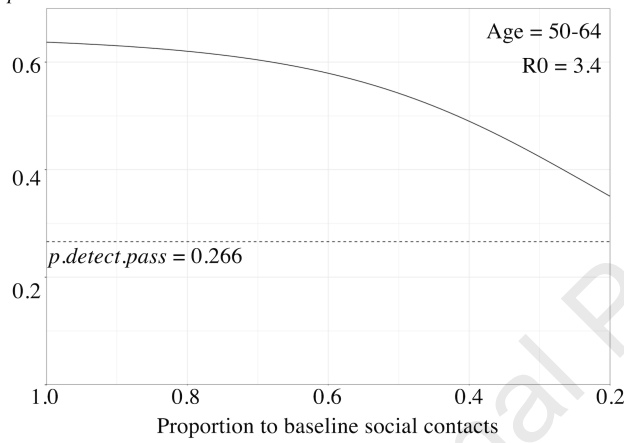
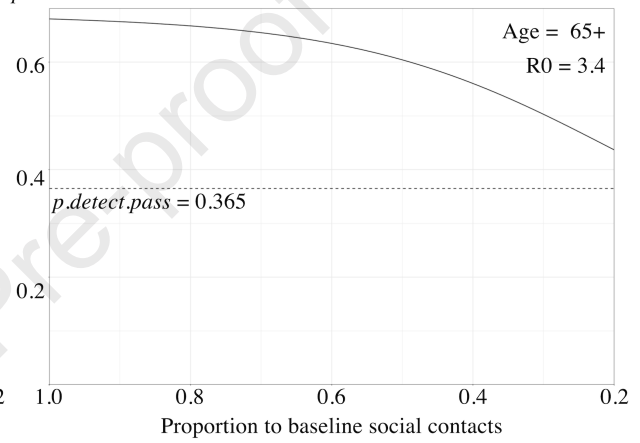
Journal Pre-proof

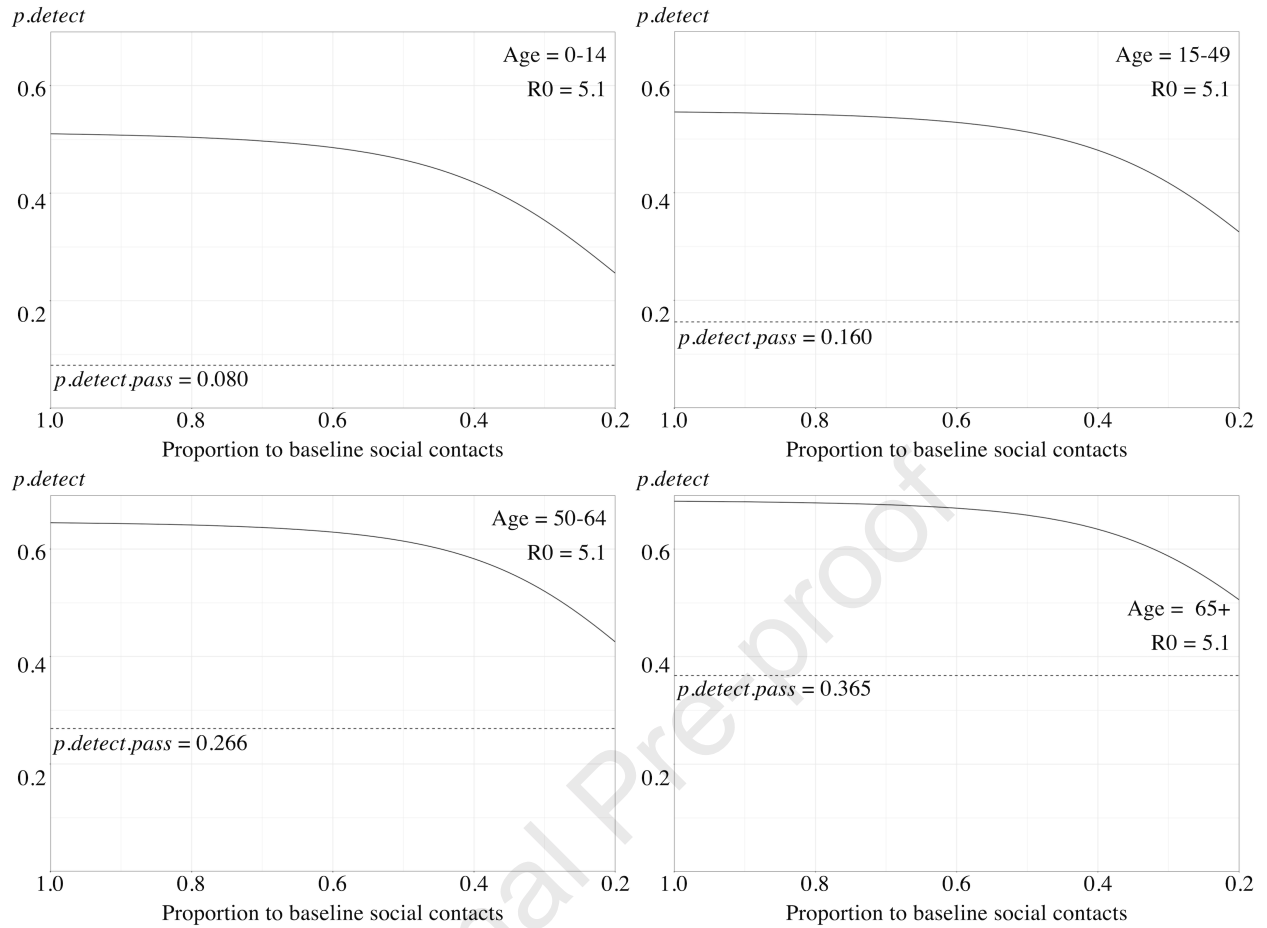


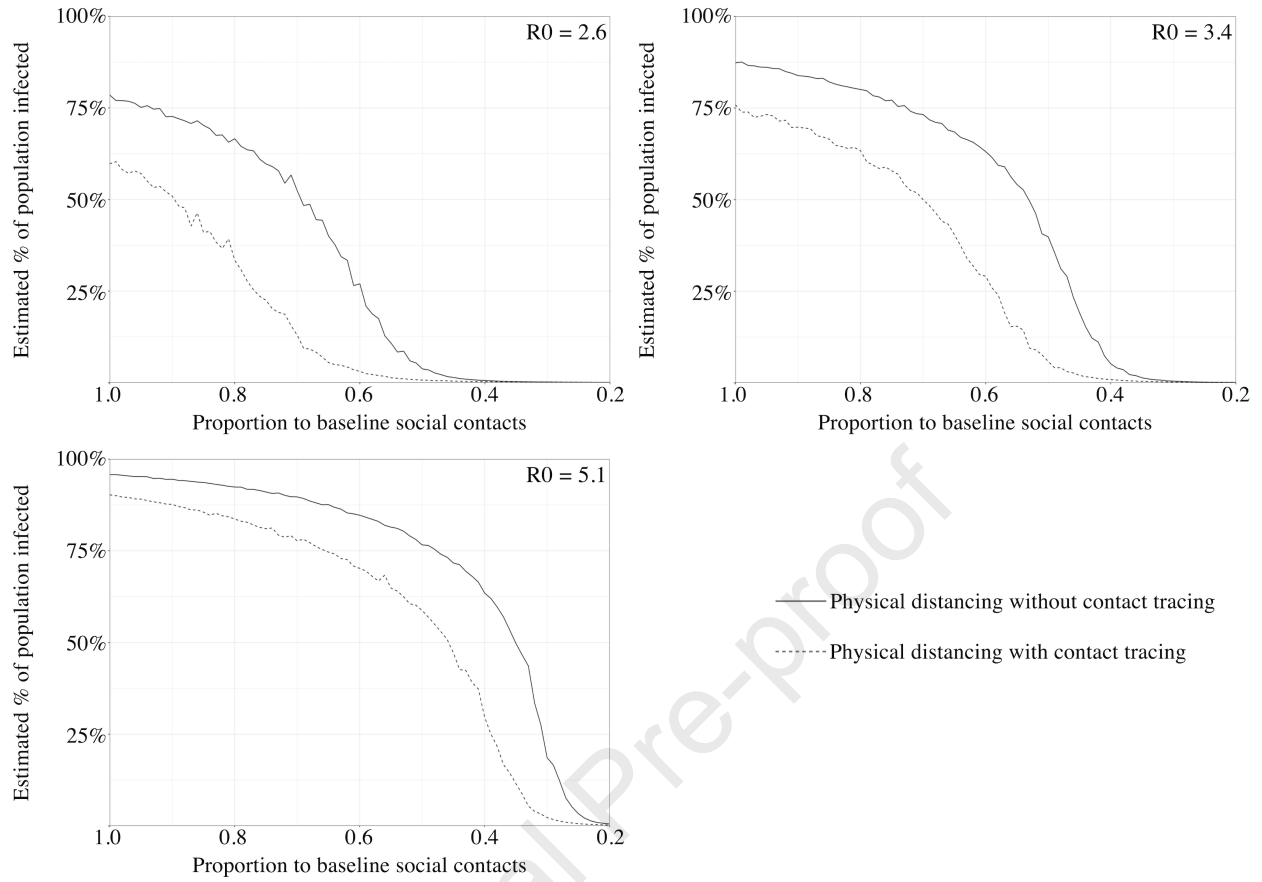






p_{detect}  p_{detect}  p_{detect}  p_{detect} 





Declaration of interests

The authors declare that they have no known competing financial interests or personal relationships that could have appeared to influence the work reported in this paper.

The authors declare the following financial interests/personal relationships which may be considered as potential competing interests:

Journal Pre-proof